Available online at www.sciencedirect.com
SCIENCE DIRECT®
Journal of Sound and Vibration 274 (2004) 529–546
JOURNAL OF SOUND AND VIBRATION
www.elsevier.com/locate/jsvi

Determination of the in-plane elastic properties of the different layers of laminated plates by means of vibration testing and model updating

T. Lauwagie[a,*], H. Sol[b], W. Heylen[a], G. Roebben[c,1]

[a] *Department of Mechanical Engineering, Katholieke Universiteit Leuven, Celestijnenlaan 300b, 3001 Heverlee, Belgium*
[b] *Department of Mechanics of Materials and Constructions, Vrije Universiteit Brussel, Pleinlaan 2, 1050 Brussels, Belgium*
[c] *Department of Metallurgy and Materials Engineering, Katholieke Universiteit Leuven, Kasteelpark Arenberg 44, 3001 Heverlee, Belgium*

Received 27 January 2003; accepted 29 May 2003

Abstract

Layered materials are becoming increasingly important for the production of high-performance components and constructions. Their stiffness properties are fundamental to assess stress fields during design calculations. Numerous analysis techniques to identify the elastic properties of materials exist, but in the case of layered materials, these techniques usually yield properties that are 'averaged' over the thickness of the test specimen. To assess the in-plane elastic properties of each individual layer, a new non-destructive testing method is developed. The proposed method derives the material properties from the resonance frequencies of a number of freely suspended test plates. A multi-model updating routine is used for this purpose. Finite element models of the different test plates are simultaneously updated. Once the Finite element models reproduce the measured frequencies, the updating procedure is halted, and the material properties of the different layers can be retrieved from the Finite element model's database. It is shown that the multi-model approach is necessary to ensure the uniqueness of the obtained properties.

1. Introduction

Elastic material properties play a major role in the vibratory behaviour of structures. This observation can be inverted, leading to the conclusion that the vibratory behaviour of samples of a particular material can be used to determine the material's elastic properties. This principle is

*Corresponding author. Fax: +32-16-32-29-87.
E-mail address: tom.lauwagie@mech.kuleuven.ac.be (T. Lauwagie).
[1] Now at Institute for Reference Materials and Measurements, Joint Research Centre of the European Commission, Retieseweg, B-2440 Geel, Belgium.

0022-460X/$ - see front matter
doi:10.1016/j.jsv.2003.05.023

the foundation of all vibration-based identification methods. An application of this principle was reported in the German 'Zeitung Für Metallkunde' by Förster in 1937 [1]. Förster used the Euler beam theory to link the elastic modulus with the specimen's eigenfrequency. In 1945 Pickett's [2] use of Goens' [3] approximate solution of the Timoshenko beam equations [4], resulted in a highly accurate relation between the elastic modulus and the fundamental transverse bending frequency of a vibrating prism or cylinder. He also introduced a relation between the shear modulus and the fundamental torsion frequency of a beam-shaped specimen. In 1961, Spinner and Teft [5] critically evaluated Pickett's formulae, and added a relation between the Young's modulus and the longitudinal vibration frequency of a prism. Their work formed the basis of the ASTM resonant beam test procedure [6], which standardized vibration testing based on these analytical relations. While the analytical formulae are derived from the differential equations of isotropic beams, resonant beam tests can still be used to identify the directional variation of the Young's modulus of orthotropic materials [7]. The use of analytical formulae to describe the vibratory behaviour of test specimens is however a major obstacle for extending the vibration methods to more complex materials. In 1986, Sol [8] showed that it is possible to replace the analytical formulae by special-purpose Finite Element (FE) models. The derived identification method, which is called the 'Resonalyser' method [9], can simultaneously identify the four engineering constants of an orthotropic material (e.g. E_1, E_2, G_{12} and ν_{12}) from measured resonance frequencies of one single test plate. During the last decade, several authors presented related approaches for the identification of orthotropic elastic constants based on resonance frequencies of thin plate specimens [10–15]. The potential to run more complex numerical models on faster computers opened the way to develop even more elaborate material identification methods. Among others, Ayorinde, Mota Soares et al., Frederiksen and Cunha extended the method to deal with transverse shear in thick plate models [16–19].

Since the introduction of composite materials, laminates have become increasingly important. In the case of these layered materials, the existing identification procedures can only yield material properties that are 'averaged' over the thickness of the specimen. In 2002, Liu et al. [20] presented a vibration based identification method that could identify the elastic properties of one single lamina of a composite plate that was made up of a number of layers of the same lamina but with different orientations of the material. However, a general identification procedure that is able to identify the properties of the individual layers of layered materials, without considering any relations between the properties of the different layers, has, to our knowledge, not yet been reported. This paper presents a novel method that is able to identify the material properties of a plate with an arbitrary number of layers, each with independent material properties. The method presented is an extension of the 'Resonalyser' procedure mentioned above for the identification of layered materials.

2. Material identification by inverse methods

2.1. The 'Resonalyser' procedure

As shown in Refs. [7–19], mixed numerical–experimental techniques (MNETs) can be used to identify the elastic properties of orthotropic materials. In a MNET a numerical model is used to

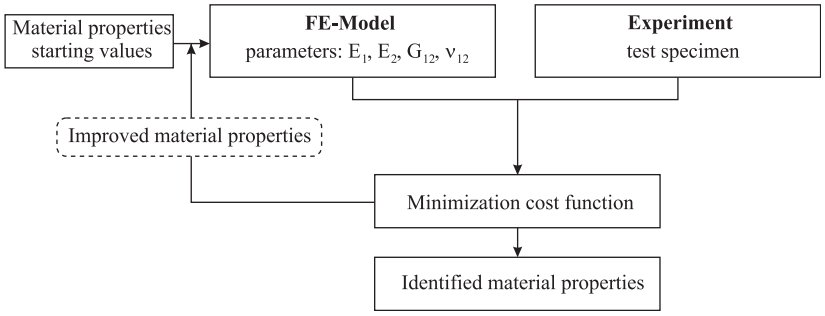

Fig. 1. General flowchart of the 'Resonalyser' procedure.

reproduce a number of experimentally measured quantities. The parameters that have to be identified are found by fine tuning these parameters in the numerical model in order to reach an optimal agreement between the measured and calculated responses. A special MNET that was developed by Sol in Ref. [8] is called the 'Resonalyser' procedure. A general flowchart of the procedure is given in Fig. 1. The 'Resonalyser' procedure uses the first five resonance frequencies of a freely suspended test plate as input data. This test configuration is used to simulate the free–free boundary conditions of the finite element model. The aspect ratio of the test plate is established in such a way that the numerical condition of the sensitivity matrix, i.e. the matrix containing the partial derivatives of the frequencies with respect to the considered elastic parameters, is good. This ensures that the sensitivity matrix can be inverted [21,22]. The resonance frequencies of the test plate are calculated with a highly accurate FE-model. The obtained frequencies are compared with the measured frequencies, and corrected material properties are found by minimizing the residues of frequency differences. The new material properties are inserted in the FE-model and a new iteration cycle is started. Once the numerical and experimental frequencies match, the procedure is aborted, and the desired material properties can be found in the database of the FE-model. This procedure has already proven to be a stable and reliable tool to identify elastic material properties [7–10]. Note that in the 'Resonalyser' procedure, the elastic material properties are considered to be homogeneous throughout the whole plate specimen.

2.2. *Non-uniqueness of the results of the 'Resonalyser' procedure applied on layered plates*

In order to identify the material properties of a layered plate, the 'Resonalyser' method was extended by taking more frequencies into account. This approach proved to be useless since it did not result in a unique solution for the layer properties. To illustrate the non-uniqueness of the obtained results, a virtual test specimen with known properties was adopted. The resonance frequencies of this virtual test specimen were computed with the finite element method. The layered test plate used was a double coated steel plate with nominal dimensions of $150 \times 150 \times 1.1$ mm. The configuration of the plate is depicted in Fig. 2, and the material properties of the different layers are given in Table 1.

The computed vibration data were next considered as 'virtual test data' and used to identify the material properties with the extended 'Resonalyser' method. The advantage of the approach with

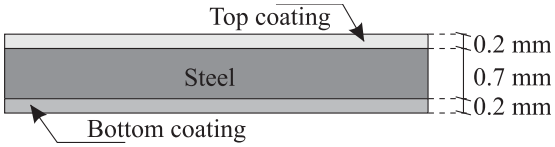

Fig. 2. Configuration of the virtual test plate.

Table 1
The material properties of the layered test plate

	E_1 (GPa)	E_2 (GPa)	G_{12} (GPa)	ν_{12} (dimensionless)	ρ (kg/m^3)
Top coating	73.00	70.00	25.00	0.340	2700
Steel	201.00	200.00	78.00	0.290	7900
Bottom coating	68.00	71.00	24.00	0.320	2700

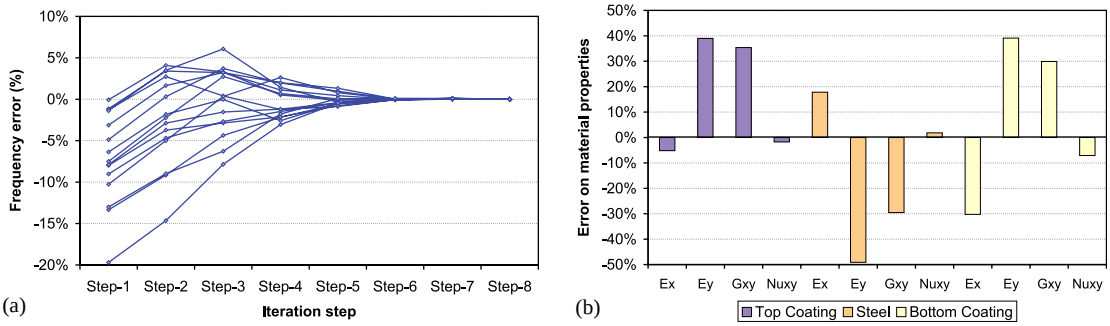

Fig. 3. (a) The frequency convergence obtained by applying the extended 'Resonalyser' method to a layered plate. (b) The convergence of the material properties obtained by applying the extended 'Resonalyser' method to a layered plate.

simulated data is that the identified material properties can be validated directly with the known properties. Since each layer is considered to be orthotropic, 12 material properties have to be identified. The original 'Resonalyser' procedure uses five frequencies to determine four material parameters: in the extended version the first 15 frequencies of the layered plate were used to identify the 12 considered material constants. The results obtained are presented in the two graphs of Fig. 3. Fig. 3a shows the frequency differences that were obtained during the different iteration steps. In eight steps, the first 15 resonance frequencies of the FE-model converged exactly to the 'experimental' frequencies. However, the obtained material properties did not match the correct properties of the test plate, as shown in Fig. 3b.

This simulation indicates that it is possible to find layered plates with completely different layer properties, but having the same resonance frequencies. The solution of the identification problem using one test plate thus appears to be non-unique.

3. The dynamical behaviour of layered plates

3.1. Classical lamination theory

In order to overcome this non-uniqueness problem, the vibratory behaviour of layered plates must be studied. The classical lamination theory (CLT) [23] is an extension of the Love–Kirchhoff thin plate theory [24] for layered materials. The main hypothesis of the Love–Kirchhoff theory is that a straight line originally perpendicular to the middle plane of the plate remains straight and flat when the plate is extended or bent. When using the notations of Fig. 4, the main Love–Kirchhoff assumption is equivalent to ignoring the deformations caused by the shearing strains γ_{xz} and γ_{yz}. Furthermore, the plate thickness is also presumed to have a constant value during loading, which means that the deformation ε_z is also ignored.

Eventually, the Love–Kirchoff hypotheses lead to the following relations between strains and displacements:

$$\begin{aligned} \varepsilon_x &= \varepsilon_x^0 + z\kappa_x, \quad \varepsilon_z = 0, \\ \varepsilon_y &= \varepsilon_y^0 + z\kappa_y, \quad \gamma_{yz} = 0, \\ \gamma_{xy} &= \gamma_{xy}^0 + z\kappa_{xy}, \quad \gamma_{xz} = 0, \end{aligned} \tag{1}$$

where ε_x^0, ε_y^0 and γ_{xy}^0 are the middle plane strains, and κ_x, κ_y, and κ_{xy} are the middle plane curvatures and are defined as

$$\varepsilon_x^0 = \frac{\partial u_0}{\partial x}, \quad \kappa_x = -\frac{\partial^2 w_0}{\partial x^2},$$

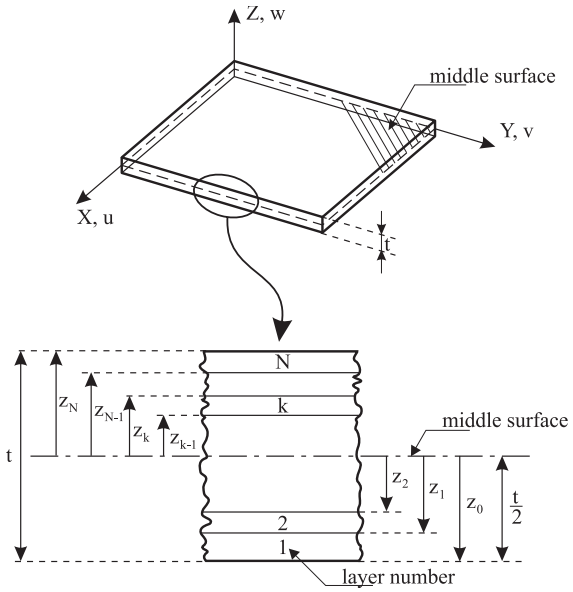

Fig. 4. Notations and conventions used by the classical lamination theory (CLT).

$$\varepsilon_y^0 = \frac{\partial v_0}{\partial y}, \quad \kappa_y = -\frac{\partial^2 w_0}{\partial y^2},$$
$$\gamma_{xy}^0 = \frac{\partial u_0}{\partial y} + \frac{\partial v_0}{\partial x}, \quad \kappa_{xy} = -2\frac{\partial^2 w_0}{\partial x\,\partial y}, \tag{2}$$

in which u_0, v_0 and w_0 are the displacements of the middle surface in the x, y and z direction respectively.

All laminae are assumed to have orthotropic material properties and are considered to be in a state of plane stress. Using these assumptions, the strains are transformed into stresses using Hooke's generalized law. The obtained stresses can be integrated over the thickness of the plate yielding Eqs. (3) and (4) for the resultant section forces N and moments M.

$$\begin{Bmatrix} N_x \\ N_y \\ N_{xy} \end{Bmatrix} = \begin{bmatrix} A_{11} & A_{12} & A_{16} \\ A_{12} & A_{22} & A_{26} \\ A_{16} & A_{26} & A_{66} \end{bmatrix} \begin{Bmatrix} \varepsilon_x^0 \\ \varepsilon_y^0 \\ \gamma_{xy}^0 \end{Bmatrix} + \begin{bmatrix} B_{11} & B_{12} & B_{16} \\ B_{12} & B_{22} & B_{26} \\ B_{16} & B_{26} & B_{66} \end{bmatrix} \begin{Bmatrix} \kappa_x \\ \kappa_y \\ \kappa_{xy} \end{Bmatrix}, \tag{3}$$

$$\begin{Bmatrix} M_x \\ M_y \\ M_{xy} \end{Bmatrix} = \begin{bmatrix} B_{11} & B_{12} & B_{16} \\ B_{12} & B_{22} & B_{26} \\ B_{16} & B_{26} & B_{66} \end{bmatrix} \begin{Bmatrix} \varepsilon_x^0 \\ \varepsilon_y^0 \\ \gamma_{xy}^0 \end{Bmatrix} + \begin{bmatrix} D_{11} & D_{12} & D_{16} \\ D_{12} & D_{22} & D_{26} \\ D_{16} & D_{26} & D_{66} \end{bmatrix} \begin{Bmatrix} \kappa_x \\ \kappa_y \\ \kappa_{xy} \end{Bmatrix} \tag{4}$$

in which the extensional stiffnesses A_{ij}, the coupling stiffnesses B_{ij}, and the bending stiffnesses D_{ij} are defined by the expressions

$$A_{ij} = \sum_{k=1}^{N} [\overline{\mathbf{Q}}_{ij}]_k (z_k - z_{k-1}),$$
$$B_{ij} = \sum_{k=1}^{N} [\overline{\mathbf{Q}}_{ij}]_k \frac{(z_k^2 - z_{k-1}^2)}{2},$$
$$D_{ij} = \sum_{k=1}^{N} [\overline{\mathbf{Q}}_{ij}]_k \frac{(z_k^3 - z_{k-1}^3)}{3}. \tag{5}$$

In Eq. (5) k represents the layer number, z_k is the transverse position of the interface between the $k-1$th and kth layer as depicted in Fig. 4. The $[\overline{\mathbf{Q}}_{ij}]_k$matrix contains the off-axis reduced stiffnesses of the kth layer. The matrix elements of $[\overline{\mathbf{Q}}_{ij}]_k$only depend the layer's orientation angle θ and the four elastic constants of the layer's material: E_1, E_2, G_{12} and ν_{12}. A more detailed overview of the classical lamination theory can be found in various textbooks on composite materials such as Ref. [23] or [25].

3.2. Differential equations of a vibrating laminated plate

Consider a differential rectangular element dx dy of a thin plate (Fig. 5). By writing the translatory and rotatory equilibria of the forces and moments acting on this differential element, the equations of motion of a vibrating plate can be obtained [25].

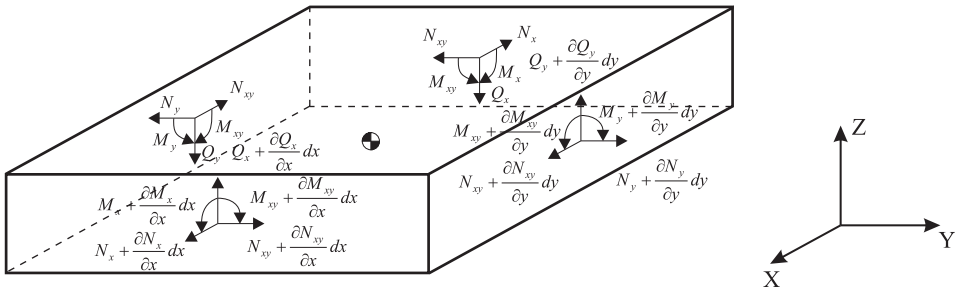

Fig. 5. Forces and moments acting on a differential rectangular element of a plate.

The translation equilibria in the x and y direction yield respectively

$$\frac{\partial N_x}{\partial x} + \frac{\partial N_{xy}}{\partial y} = \rho t \frac{\partial^2 u_0}{\partial t^2}, \tag{6}$$

$$\frac{\partial N_y}{\partial y} + \frac{\partial N_{xy}}{\partial x} = \rho t \frac{\partial^2 v_0}{\partial t^2}, \tag{7}$$

where ρ is the mass density of the plate's material, and t is the total plate thickness.

By inserting the rotation equilibrium equations with respect to the X- and Y-axis into the translation equilibrium equation in the z direction, expression (8) is obtained.

$$\frac{\partial^2 M_x}{\partial x^2} + 2\frac{\partial^2 M_{xy}}{\partial x\,\partial y} + \frac{\partial^2 M_y}{\partial y^2} = \rho t \frac{\partial^2 w_0}{\partial t^2}. \tag{8}$$

Note that the effects of rotatory inertia were neglected, and that no volume forces were considered during the derivation of these three equilibrium equations. Inserting expressions (3) and (4) into Eqs. (6)–(8) yields a set of three partial differential equations (9)–(11), describing the vibratory behaviour of laminated plates.

$$\begin{aligned} &A_{11}\frac{\partial^2 u_0}{\partial x^2} + 2A_{16}\frac{\partial^2 u_0}{\partial x\,\partial y} + A_{66}\frac{\partial^2 u_0}{\partial y^2} + A_{16}\frac{\partial^2 v_0}{\partial x^2} + (A_{12}+A_{66})\frac{\partial^2 v_0}{\partial x\,\partial y} + A_{26}\frac{\partial^2 v_0}{\partial y^2} \\ &- B_{11}\frac{\partial^3 w_0}{\partial x^3} - 3B_{16}\frac{\partial^3 w_0}{\partial x^2\,\partial y} - (B_{12}+2B_{66})\frac{\partial^3 w_0}{\partial x\,\partial y^2} - B_{26}\frac{\partial^3 w_0}{\partial y^3} = \rho t \frac{\partial^2 u_0}{\partial t^2}, \end{aligned} \tag{9}$$

$$\begin{aligned} &A_{16}\frac{\partial^2 u_0}{\partial x^2} + (A_{12}+A_{66})\frac{\partial^2 u_0}{\partial x\,\partial y} + A_{26}\frac{\partial^2 u_0}{\partial y^2} + A_{66}\frac{\partial^2 v_0}{\partial x^2} + 2A_{26}\frac{\partial^2 v_0}{\partial x\,\partial y} + A_{22}\frac{\partial^2 v_0}{\partial y^2}, \\ &- B_{16}\frac{\partial^3 w_0}{\partial x^3} - (B_{12}+2B_{66})\frac{\partial^3 w_0}{\partial x^2\,\partial y} - 3B_{26}\frac{\partial^3 w_0}{\partial x\,\partial y^2} - B_{22}\frac{\partial^3 w_0}{\partial y^3} = \rho t \frac{\partial^2 v_0}{\partial t^2}, \end{aligned} \tag{10}$$

$$D_{11}\frac{\partial^4 w_0}{\partial x^4} + 4D_{16}\frac{\partial^4 w_0}{\partial x^3\,\partial y} + 2(D_{12}+2D_{66})\frac{\partial^4 w_0}{\partial x^2\,\partial y^2} + 4D_{26}\frac{\partial^4 w_0}{\partial x\,\partial y^3} + D_{22}\frac{\partial^4 w_0}{\partial y^4}$$
$$- B_{11}\frac{\partial^3 u_0}{\partial x^3} - 3B_{16}\frac{\partial^3 u_0}{\partial x^2\,\partial y} - (B_{12}+2B_{66})\frac{\partial^3 u_0}{\partial x\,\partial y^2} - B_{26}\frac{\partial^3 u_0}{\partial y^3}$$
$$- B_{16}\frac{\partial^3 v_0}{\partial x^3} - (B_{12}+2B_{66})\frac{\partial^3 v_0}{\partial x^2\,\partial y} - 3B_{26}\frac{\partial^3 v_0}{\partial x\,\partial y^2} - B_{22}\frac{\partial^3 v_0}{\partial y^3} = \rho t\frac{\partial^2 w_0}{\partial t^2}. \quad (11)$$

3.3. Discussion

Solving the set partial differential equations (9)–(11) in combination with the appropriate boundary condition equations, yields the resonance frequencies and mode shapes of the considered laminated plate. The boundary condition equations are functions of N_x, N_y, N_{xy}, M_x, M_y and M_{xy}, and can therefore only depend on the plate's material properties via the A_{ij}, B_{ij} and D_{ij} stiffness coefficients. This shows that the modal parameters of a laminated plate are not a function of the material properties of the individual layers, but that the dynamical behaviour is entirely controlled by the integrated stiffnesses defined by the A_{ij}, B_{ij} and D_{ij} stiffness coefficients. Two plates with the same dimensions and weight, but made up with a completely different set of layers, will dynamically respond identically if they have the same A_{ij}, B_{ij} and D_{ij} stiffness coefficients.

From an identification point of view, this observation implies that only the values of the A_{ij}, B_{ij} and D_{ij} coefficients can be obtained from the measured vibration data of a laminated plate. Since the A, B and D matrices are symmetric, there are 18 identifiable coefficients. In the case of orthotropic laminae, the reduced stiffnesses Q_{16} and Q_{26} depend on the values of Q_{11}, Q_{12}, Q_{22} and Q_{66}, and therefore the X_{16} and X_{26} coefficients—with X representing A, B or D—depend on X_{11}, X_{22}, X_{12} and X_{66} coefficients, reducing the total number of independent plate stiffness coefficients to 12. Since the modal data of an arbitrary laminated plate is entirely controlled by 12 independent coefficients, only 12 independent equations linking the material properties of the plate to the measured modal quantities can be written. Because the layers of the plate are considered to have orthotropic material properties, these 12 equations can only yield the material properties of three layers.

This maximum of three layers is a theoretical limit. In the case of real experiments the number of identifiable layers will be lower, since only frequencies of transverse modes are measured. These transverse modes are insensitive to changes in the extensional stiffnesses A_{ij}, and the effects of changes in the coupling stiffness B_{ij} are also limited. So, in most practical cases, only the values of the bending stiffnesses D_{ij} can be identified with sufficient accuracy, reducing the number of identifiable layers to one single layer.

3.4. Example

This example will illustrate the insensitivity of the first 10 frequencies of a layered plate for changes of the extensional stiffnesses A_{ij} and the coupling stiffnesses B_{ij}. Consider once again the virtual test plate described in Section 2.2. The material properties of the third layer were replaced

Table 2
The properties of the equivalent plate

	E_1 (GPa)	E_2 (GPa)	G_{12} (GPa)	ν_{12} (dimensionless)	Status
Layer 1	52.10	97.83	32.00	0.313	Optimized
Layer 2	261.50	95.92	57.84	0.324	Optimized
Layer 3	47.00	98.00	31.00	0.300	Fixed

Table 3
The differences between the plate stiffnesses of the initial and equivalent plate

	Difference (%)		Difference (%)		Difference (%)
A_{11}	−15.946	B_{11}	−0.415	D_{11}	0.000
A_{22}	36.053	B_{22}	−0.122	D_{22}	0.000
A_{12}	31.729	B_{12}	0.622	D_{12}	0.000
A_{66}	17.566	B_{66}	0.220	D_{66}	0.000

with the following set of arbitrary chosen values: $E_1 = 47\,\text{GPa}$, $E_2 = 98\,\text{GPa}$, $G_{12} = 31\,\text{GPa}$, $\nu_{12} = 0.3$. Next the elastic properties of the first two layers were optimized in such a way that the A, B and D stiffness coefficients matched the stiffness coefficients of the initial plate as closely as possible. The optimization approach is needed since there are only three layers which makes it impossible to find a complete match between the two sets of plate stiffnesses. Because the transverse vibrations are mainly controlled by the values of the bending stiffnesses, the optimization focused on matching the D coefficients. The optimal layer properties are given in Table 2 and were found by inserting the values of the stiffness coefficients of the initial plate, together with the arbitrary chosen values of the elastic properties of the third layer into the expressions of Eq. (5). This resulted in a set of 12 equations with eight independent unknowns. The eight independent unknowns are the elastic properties of the first two layers. An optimal solution to this set of equations was obtained in a least-squares way where the residuals of the bending stiffness coefficients D_{ij} were weighted with a factor 1000 compared to the weighting of the A_{ij} and B_{ij} stiffness coefficients. Table 2 shows the obtained material properties and Table 3 gives the differences between the values of the 12 plate stiffnesses of the initial and the equivalent plates.

Inspection of Tables 2 and 3 shows that it is possible to find a plate with completely different material properties for its layers—differences up to 52%—that will result in the same bending stiffnesses. The bending stiffnesses D_{ij} are completely matched, the match of the coupling stiffnesses B_{ij} is acceptable, while the match of the extensional stiffnesses A_{ij} is poor. However, when the first 10 resonance frequencies—all of them are associated with transverse vibration modes—are calculated, a perfect match between the frequencies of the initial and equivalent plate is found (Table 4). This simple example shows very clearly that the transverse vibration modes are only sufficiently sensitive to changes of the bending stiffnesses, and that it is therefore impossible to identify the material properties of the individual layers of layered material from the transverse vibrations of one single test plate.

Table 4
Comparison between the first 10 resonance frequencies of the initial and equivalent plate

Mode	Original	Equivalent	Difference (%)
1	129.277	129.276	0.000
2	191.575	191.576	0.000
3	239.097	239.098	−0.001
4	336.919	336.918	0.000
5	337.068	337.069	0.000
6	600.046	600.046	0.000
7	600.747	600.751	−0.001
8	615.731	615.731	0.000
9	674.085	674.085	0.000
10	754.527	754.529	0.000

Table 5
The differences between the correct plate stiffnesses and the stiffnesses identified by the extended 'Resonalyser' method

	Difference (%)		Difference (%)		Difference (%)
A_{11}	−8.1	B_{11}	−463.3	D_{11}	−0.4
A_{22}	34.2	B_{22}	−916.4	D_{22}	−0.1
A_{12}	31.9	B_{12}	−479.5	D_{12}	−0.3
A_{66}	20.1	B_{66}	−351.5	D_{66}	0.0

Table 5 compares the plate stiffnesses of the test plate with the plate stiffnesses obtained with the material properties that were identified using the extended 'Resonalyser' method in Section 2.2. The comparison confirms that transverse vibrations of a plate only contain useful information about the bending stiffnesses.

4. Identifying the layer properties

4.1. The 'multi-model Resonalyser' procedure

The vibration data obtained from one single plate do not supply enough information to identify the material properties of the different layers of the laminate. The amount of available test data can be increased by measuring frequencies on a number of additional test plates. The vibration data of each plate are controlled by the integrated through-thickness stiffness. To decompose these integrated stiffnesses into the individual layer stiffnesses, different sets of integrated plate stiffnesses, in which the contribution of the individual layers varies, are needed. Eqs. (5) and (9)–(11) show that changing the size or shape of the test plates is useless, since their vibration data will still be controlled by the same set of plate stiffnesses A_{ij}, B_{ij} and D_{ij}. From the expressions in Eq. (5) it can be seen that the plate stiffnesses can only be altered by changing the layer thicknesses or the stacking sequence.

Varying the stacking sequence will not be considered because this sequence is usually fixed by the production system. One possibility to create altered plate stiffnesses, is to remove a layer of the

specimen. While this is physically possible in some cases, the experience of the authors has shown that this is a very inconvenient way of working. The considered layer must be removed very carefully to ensure that the remaining layers are not damaged. Another main disadvantage of this technique is its destructive character. Alternatively, the contribution of the individual layers to the total plate stiffnesses can be changed by adding one or more layers with known stiffness properties to the laminate. Additional layers can be 'glued' to the test plate. The test method becomes non-destructive if the added layer can be removed after testing. Adding a layer to a system is relatively easy and does not require expensive equipment. Each new plate provides four new bending stiffnesses while no new unknown parameters are introduced.

Since each layer is considered to be orthotropic and can thus be described by four material parameters, the total number of parameters that must be identified becomes $4 \times$ 'the number of different materials used in the layers of the laminate' $(= n_m)$. Because each plate provides four equations relating the measured plate bending stiffnesses to the material properties, the minimum number of plates that is needed to identify the material properties becomes n_m. So, the original test plate will have to be measured with $n_m - 1$ additional plate configurations. Different configurations can be obtained by adding layers made of different materials or with different thicknesses. In the case of non-symmetric laminates, different plates can be obtained by adding the same layer to the top or to the bottom side of the original plate. Note, that the number of possible configurations is virtually unlimited, therefore the 'multi-model Resonalyser' procedure could also be used to identify the material properties of gradient materials by modelling the gradient with a discrete number of uniform layers. Finally, it should be added that the mass densities of the different layers do not have to be known. As in the case of the stiffness properties, the vibratory behaviour of the layered plate only depends on the integrated mass properties of the plate. The identification procedure can be executed by replacing the real mass densities of the different layers by the average mass density of the laminate without influencing the obtained results.

4.2. The multi-model the identification procedure

Fig. 6 presents the detailed flowchart of the multi-model version of the 'Resonalyser' procedure for the identification of the elastic properties of the layers. The first five resonance frequencies of the test plate are measured with n_c plate configurations (including the original configuration), with $n_c \geqslant n_m$. In order to simulate the free–free boundary conditions of the FE-models as closely as possible, all the test plates are suspended with very thin wires during the vibration tests. For each plate configuration, a FE-model is created, and the resonance frequencies are calculated from a set of estimated initial values for the material parameters. The mass and geometry of the test plates are considered to be known, and the differences between the measured and calculated frequencies are assumed to be caused entirely by the incorrect values of the elastic properties used for the materials of the different FE-models. For each plate the relative frequency differences and normalized relative frequency sensitivities [26] are calculated, yielding the following set of equations:

$$\{\mathbf{\Delta R}\}_k = [\mathrm{S}]_k \{\mathbf{\Delta P}\}, \tag{12}$$

where $\{\mathbf{\Delta R}\}_k \in \mathrm{R}^{5\times 1}$ contains the relative frequency differences of the first five modes of the plate with the kth configuration, and the vector $\{\mathbf{\Delta P}\} \in \mathrm{R}^{4\times n_m}$ contains the relative parameter changes of different material properties. The matrix $[\mathbf{S}]_k \in \mathrm{R}^{5\times(4\times n_m)}$ is the sensitivity matrix of the plate with

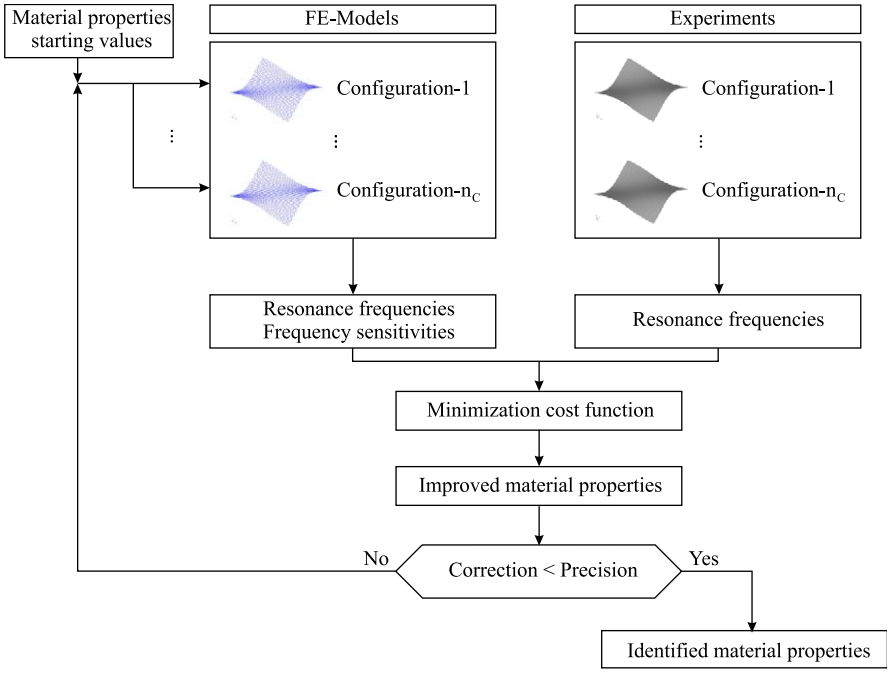

Fig. 6. The detailed flowchart of the multi-layer version of the Resonalyser procedure.

the kth configuration: the calculation of this matrix is discussed in Section 4.4. Mathematically the three components of Eq. (12) are expressed as

$$\{\Delta\mathbf{R}\}_k = \begin{Bmatrix} \frac{f_{exp,1}-f_{FE,1}^{(p)}}{f_{exp,1}} \\ \vdots \\ \frac{f_{exp,5}-f_{FE,5}^{(p)}}{f_{exp,5}} \end{Bmatrix}_k \quad \text{and}$$

$$\{\Delta\mathbf{P}\} = \left\{ \overbrace{\frac{E_{1,1}^{(p+1)}-E_{1,1}^{(p)}}{E_{1,1}^{(p)}} \quad \cdots \quad \frac{v_{12,1}^{(p+1)}-v_{12,1}^{(p)}}{v_{12,1}^{(p)}}}^{Material\ 1} \quad \cdots \quad \overbrace{\frac{E_{1,n_m}^{(p+1)}-E_{1,n_m}^{(p)}}{E_{1,n_m}^{(p)}} \quad \cdots \quad \frac{v_{12,n_m}^{(p+1)}-v_{12,n_m}^{(p)}}{v_{12,n_m}^{(p)}}}^{Material\ n_m} \right\}^{\mathrm{T}},$$

$$[\mathbf{S}]_k = \left[\overbrace{\begin{matrix} \frac{\partial f_1}{\partial E_{1,1}}\frac{E_{1,1}}{f_1} & \frac{\partial f_1}{\partial E_{2,1}}\frac{E_{2,1}}{f_1} & \frac{\partial f_1}{\partial G_{12,1}}\frac{G_{12,1}}{f_1} & \frac{\partial f_1}{\partial v_{12,1}}\frac{v_{12,1}}{f_1} \\ \frac{\partial f_2}{\partial E_{1,1}}\frac{E_{1,1}}{f_2} & \frac{\partial f_2}{\partial E_{2,1}}\frac{E_{2,1}}{f_2} & \frac{\partial f_2}{\partial G_{12,1}}\frac{G_{12,1}}{f_2} & \frac{\partial f_2}{\partial v_{12,1}}\frac{v_{12,1}}{f_2} \\ \vdots & \vdots & \vdots & \vdots \\ \frac{\partial f_5}{\partial E_{1,1}}\frac{E_{1,1}}{f_5} & \frac{\partial f_5}{\partial E_{2,1}}\frac{E_{2,1}}{f_5} & \frac{\partial f_5}{\partial G_{12,1}}\frac{G_{12,1}}{f_5} & \frac{\partial f_5}{\partial v_{12,1}}\frac{v_{12,1}}{f_5} \end{matrix}}^{Material\ 1} \quad \cdots \quad \overbrace{\begin{matrix} \frac{\partial f_1}{\partial E_{1,n_m}}\frac{E_{1,n_m}}{f_1} & \frac{\partial f_1}{\partial E_{2,n_m}}\frac{E_{2,n_m}}{f_1} & \frac{\partial f_1}{\partial G_{12,n_m}}\frac{G_{12,n_m}}{f_1} & \frac{\partial f_1}{\partial v_{12,n_m}}\frac{v_{12,n_m}}{f_1} \\ \frac{\partial f_2}{\partial E_{1,n_m}}\frac{E_{1,n_m}}{f_2} & \frac{\partial f_2}{\partial E_{2,n_m}}\frac{E_{2,n_m}}{f_2} & \frac{\partial f_2}{\partial G_{12,n_m}}\frac{G_{12,n_m}}{f_2} & \frac{\partial f_2}{\partial v_{12,n_m}}\frac{v_{12,n_m}}{f_2} \\ \vdots & \vdots & \vdots & \vdots \\ \frac{\partial f_5}{\partial E_{1,n_m}}\frac{E_{1,n_m}}{f_5} & \frac{\partial f_5}{\partial E_{2,n_m}}\frac{E_{2,n_m}}{f_5} & \frac{\partial f_5}{\partial G_{12,n_m}}\frac{G_{12,n_m}}{f_5} & \frac{\partial f_5}{\partial v_{12,n_m}}\frac{v_{12,n_m}}{f_5} \end{matrix}}^{Material\ n_m} \right]_k^{(p)}, \tag{13}$$

where $[\blacklozenge]^{\mathrm{T}}$ is the transpose of a matrix, and $E_{1,i}^{(p)}$ denotes the E_1 modulus of the ith material, during the pth iteration cycle.

For each configuration a set of equations like Eq. (12) is obtained, and these n_c sets can be combined into one global set of equations:

$$\underbrace{\begin{Bmatrix} \Delta R_1 \\ \Delta R_2 \\ \vdots \\ \Delta R_{n_c} \end{Bmatrix}}_{\{\Delta\mathbf{R}\}} = \underbrace{\begin{bmatrix} S_1 \\ S_2 \\ \vdots \\ S_{n_c} \end{bmatrix}}_{[\mathbf{S}]} \{\Delta\mathbf{P}\}, \tag{14}$$

where $\{\Delta\mathbf{R}\} \in \mathrm{R}^{5\times n_c}$ is the global relative frequency difference vector and $[\mathbf{S}] \in \mathrm{R}^{(5\times n_c)\times(4\times n_m)}$ is the global sensitivity matrix. The improved material properties can be found by solving the system of equations (14) in a least-squares sense:

$$\{\Delta\mathbf{P}\} = [\mathbf{S}]^{\dagger}\{\Delta\mathbf{R}\} \tag{15}$$

in which $[\mathbf{S}]^{\dagger}$ denotes the Moore–Penrose pseudo-inverse of $[\mathbf{S}]$. If the obtained corrections of the material properties are smaller than a selected convergency criterion, the procedure has converged and the identified material properties are found in the databases of the FE-models. If not, the improved material properties are introduced into the various FE-models and a new iteration is started.

4.3. Selection of the used frequencies and specimen shape

The application of the multi-layer identification method presented in the previous paragraph requires five resonance frequencies of the different test specimen configurations. The five experimental frequencies that are used cannot be chosen arbitrarily. A useful frequency set has to be sensitive to all material parameters. Bending and torsion modes are sensitive to Young's and shear moduli respectively. But these modes are very insensitive to changes of the Poisson ratio. To obtain modes that are sufficiently sensitive to the Poisson ratio, test plates with a particular length to width ratio have to be used [8]. If the length-to-width ratio complies with Eq. (16), the frequencies of the first bending modes in the x and y direction coincide. The two bending modes will interact, and will form two new modes: an 'anticlastic' and 'synclastic' mode (Fig. 7).

$$\frac{length}{width} = \sqrt[4]{\frac{E_1}{E_2}}. \tag{16}$$

The anticlastic mode is the combination with a 180° phase difference between the two bending modes, and the synclastic mode is the in-phase combination of the two bending modes. Because of the high Poisson ratio sensitivity, a plate of which the length to width ratio complies with (16) is called a Poisson plate. Fig. 7 gives an overview of the material parameters to which the different frequencies of a Poisson plate are sensitive. In this set there is a sensitivity to all the material parameters, and the first five modes thus provide a usable frequency set. Note that the first four modes provide enough information to identify the material parameters, but five frequencies are preferred since this results in an overdetermined set of equations.

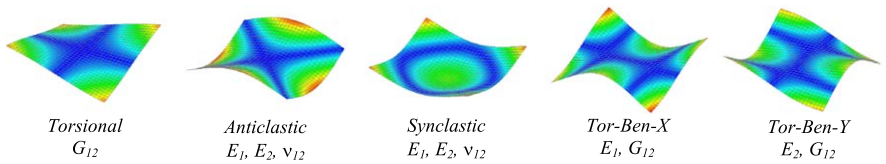

Fig. 7. The mode shapes of the first five modes of a Poisson test plate. The frequencies associated with these modes are mainly sensitive to the material parameters indicated under the mode shapes.

4.4. Sensitivity analysis

Sensitivity analysis is a technique that determines the rate of change of modal parameters due to mass, damping or stiffness changes. It is an excellent tool to estimate the amount of modification needed to achieve a desired change of the dynamic behaviour of a finite element model. A sensitivity analysis results in a number of sensitivity coefficients, which can be grouped into a sensitivity matrix. Sensitivity coefficients are defined as the rate of change of a particular response quantity r with respect to a change of a model parameter p.

In structural dynamics there are two major approaches for the computation of the sensitivity coefficients: the finite difference and the differential approach. With the finite difference approach the partial derivatives of the model parameters are numerically approximated, by using the outputs of two FE-models in which one parameter is slightly altered:

$$\frac{\partial r_i(p_j)}{\partial p_j} \approx \frac{r_i(p_j + \Delta p_j) - r_i(p_j)}{\Delta p_j}. \tag{17}$$

The calculation of the sensitivity coefficients for a particular model parameter, thus requires an extra evaluation of the FE-model, which makes this approach very time consuming.

Differential sensitivity calculation is based on explicit expressions of the partial derivatives of the FE-responses. The expression for the differential frequency sensitivities for undamped systems was established by Fox and Kapoor [27]. In the case where only stiffness changes are considered the frequency sensitivity can be expressed as

$$\frac{\partial f_i}{\partial p} = \frac{1}{8\pi^2 f_i} \sum_{e=1}^{n_e} \left(\{\mathbf{\Psi_e}\}_i^{\mathrm{T}} \frac{\partial [\mathbf{K_e}]}{\partial p} \{\mathbf{\Psi_e}\}_i \right) \tag{18}$$

in which f_i is the resonance frequency associated with the ith mode, n_e is the number of elements of the FE-model, $[\mathbf{K_e}]$ is the stiffness matrix of the eth element, and $\{\mathbf{\Psi}_e\}_i$ contains the modal displacements of the nodes of the eth element for the ith vibration mode. In the case of orthotropic materials, the partial derivative of the element matrices has to be estimated with a finite difference approach. But the calculation of the sensitivity coefficients with Eq. (18) will be considerably faster than with the finite difference approach, because the computation of element matrices take less time than solving a FE-model. In the case of the identification method considered here, the sensitivity calculation (18) can be simplified even more. Eq. (18) shows that the sensitivity coefficients are the sum of the element sensitivity contributions. It can be shown that a FE-model of a homogeneous plate has two symmetry axes for the element sensitivity contributions. The sensitivity coefficients can thus be calculated by considering only one-quarter

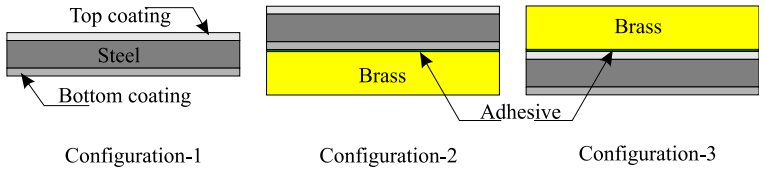

Fig. 8. The three different plate configurations.

Table 6
The evolution of the material properties during the updating

		Correct	Start	Step-1	Step-2	Step-3	Step-4
Layer-1	E_x	73.00	151.00 (107%)	75.50 (3%)	74.38 (2%)	73.02 (0%)	73.00 (0%)
	E_y	70.00	150.00 (114%)	75.00 (7%)	71.24 (2%)	70.02 (0%)	70.00 (0%)
	G_{xy}	25.00	50.00 (100%)	25.00 (0%)	25.04 (0%)	25.00 (0%)	25.00 (0%)
	v_{xy}	0.34	0.25 (−26%)	0.27 (−21%)	0.33 (−4%)	0.34 (0%)	0.34 (0%)
Layer-2	E_x	201.00	151.00 (−25%)	166.79 (−17%)	197.51 (−2%)	200.99 (0%)	201.00 (0%)
	E_y	200.00	150.00 (−25%)	173.58 (−13%)	198.19 (−1%)	200.01 (0%)	200.00 (0%)
	G_{xy}	78.00	50.00 (−36%)	72.83 (−7%)	77.73 (0%)	78.00 (0%)	78.00 (0%)
	v_{xy}	0.29	0.25 (−14%)	0.38 (29%)	0.30 (3%)	0.29 (0%)	0.29 (0%)
Layer-3	E_x	68.00	151.00 (122%)	75.50 (11%)	69.91 (3%)	68.03 (0%)	68.00 (0%)
	E_y	71.00	150.00 (111%)	75.00 (6%)	72.47 (2%)	71.03 (0%)	71.00 (0%)
	G_{xy}	24.00	50.00 (108%)	25.00 (4%)	24.10 (0%)	24.00 (0%)	24.00 (0%)
	v_{xy}	0.32	0.25 (−22%)	0.26 (−20%)	0.31 (−4%)	0.32 (0%)	0.32 (0%)

of the plate:

$$\frac{\partial f_i}{\partial p} = \frac{4}{8\pi^2 f_i} \sum_{e=1}^{n_e/4} \left(\{\boldsymbol{\Psi}_\mathbf{e}\}_i^{\mathrm{T}} \frac{\partial [\mathbf{K}_\mathbf{e}]}{\partial p} \{\boldsymbol{\Psi}_\mathbf{e}\}_i \right) \tag{19}$$

which reduces the computation time of the sensitivity analysis by a factor four.

4.5. Example of the multi-model identification procedure

To illustrate the performance of the proposed identification method, the material properties of the double coated steel plate described in Section 2.2. will be identified. The total thickness of 1.1 mm is composed by two thicknesses of the coating layers of 0.2 mm each and a steel layer of 0.7 mm thickness. Since there are three different layers, the test plate will have to be measured in three different configurations. The configurations are sketched in Fig. 8. The first configuration was the initial test plate. The second configuration was obtained by sticking a 1 mm thick brass plate to the bottom surface of the test plate. The adhesive layer was assumed to have a thickness of 50 μm. For the last configuration the brass plate was removed from the bottom surface and next fixed to top surface of the test plate. The material properties of the brass and adhesive were considered as known quantities.

Initially, the first five resonance frequencies of the three configurations of the test plate were calculated using finite element models. In a second stage the material properties of the steel and the two coatings were considered to be unknown, and their values were set to the starting values

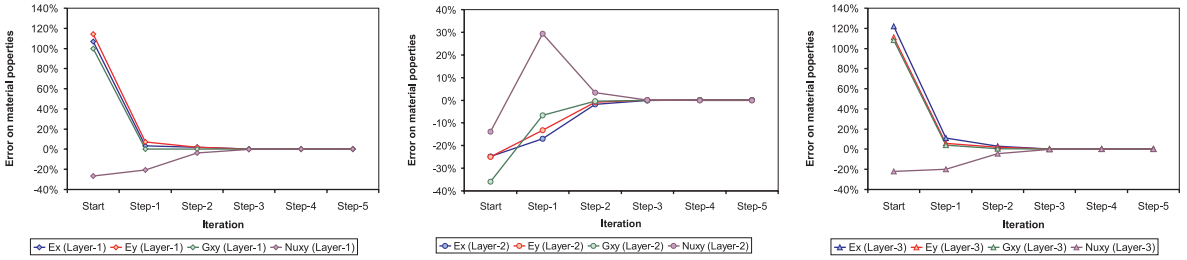

Fig. 9. The convergence sequences of the properties of the top coating (left), steel substrate (middle) and bottom coating (right).

given in Table 6. The three finite element models were simultaneously updated in order to obtain a match between the 'measured' resonance frequencies and the calculated frequencies according to the procedure described in Section 4.2. The iteration sequences and the obtained material properties are given in Table 6 and Fig. 9. Only three iterations were needed to find the correct material properties of the different layers.

4.6. Discussion of the identifiability condition

The failure of the single plate procedure to identify the correct material properties is obvious considering the conclusions of Section 3. The non-identifiability can also be assessed in an alternative way. In Ref. [28] it is stated that in identification problems "parameters cannot be uniquely identified if the sensitivity coefficients are linearly dependent". This identifiability condition holds under the assumptions that the objective function used to estimate the parameters is formed by some least-squares function, that the sensitivities are continuous functions of the parameters, and that there is no prior information regarding the parameters.

In the case of an identification procedure with one single test plate, the sensitivity coefficients of the first column of the global sensitivity matrix can be expressed as a linear combination of the sensitivity coefficients of the other 11 columns. This is presented in Fig. 10a, where the x-co-ordinate of each point is the sensitivity coefficient of the first column, and the y-co-ordinate is a linear combination of the sensitivity coefficients of the other columns. Fig. 10a shows that the sensitivity matrix of the routine with one single plate does not comply with the identifiability condition, since the sensitivity coefficients are clearly not independent. Fig. 10b shows the relation between the columns of the global sensitivity matrix of the example where three plate configurations were used. The first column of the global sensitivity matrix cannot be expressed as a linear combination of the other columns, which proves once again that multiple plate configurations are needed to identify the material properties of the individual layers.

The linear dependency of the columns of a matrix can also be investigated by means of the matrix condition number. The condition number is the ratio of the largest over the smallest singular value of a matrix, and varies between 1 and ∞. Large condition numbers indicate ill-conditioned or singular matrices. For example, where only one plate was used, the global sensitivity matrix had a condition number of 6.76e9, while the condition number of the sensitivity matrix of the three plate routine was only 34.4. In Ref. [29], it is stated that updating problems with condition numbers larger than 10^3 can be considered as ill-conditioned, and that problems

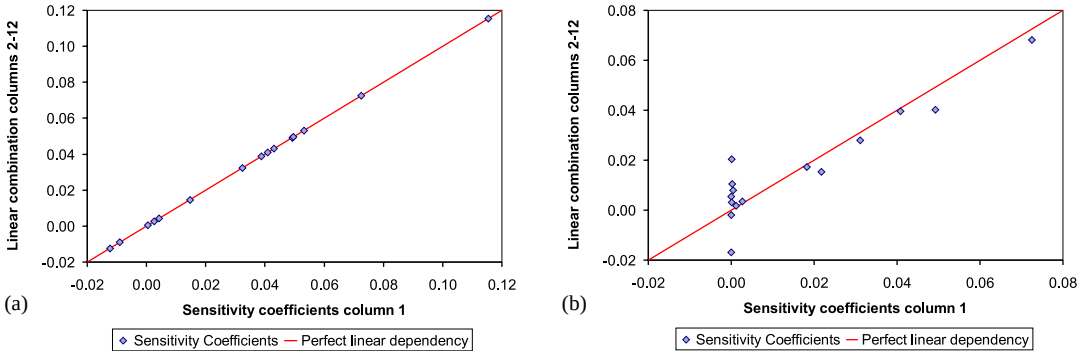

Fig. 10. Linear dependency of the sensitivity coefficients of the procedure using one single test plate (a) and of the procedure using three different plate configurations (b).

with condition numbers larger than 10^7 are to be considered singular and should subsequently be avoided. The condition number can be used as a pre-test investigation tool to check if the proposed plate modifications are large enough and if the considered plate configurations will lead to a stable and successful identification procedure. In this way valuable time can be saved.

5. Conclusions

This paper has shown that it is impossible to identify the elastic material properties of the individual layers of a laminate from the vibration data of one single test specimen. To identify the material properties of the different layers, the vibration data of a number of test plates with different plate stiffnesses is necessary. Creation of test plates with different stiffness values by adding layers with known material properties was proposed as a solution for this problem. A mixed numerical–experimental identification method based on this principle, using the first five resonance frequencies of freely suspended test plates with different configurations as input data, was presented. The identification procedure was evaluated by means of a numerically simulated experiment, and proved to be a promising tool to identify the orthotropic material properties of the individual layers of a laminate.

Acknowledgements

This work was performed in the framework of the GRAMATIC research project supported by the Flemish Institute for the Promotion of Scientific and Technological Research in Industry IWT. Gert Roebben is a postdoctoral fellow of the FWO-Vlaanderen.

References

[1] F. Förster, Ein neues Messverfahren zur Bestimmung des Elastizitäts-moduls und der Dämpfung, *Zeitschrift füer Metallkunde* 29 (1937) 109–115.

[2] G. Pickett, Equations for computing elastic constants from flexural and torsional resonant frequencies of vibrating prisms and cylinders, *Proceedings of the ASTM*, Vol. 45, 1945, pp. 846–865.

[3] E. Goens, Über die Bestimmung des Elastizitätsmodulus von Stäben mit Hilfe von Biegungsschwingungen, *Annalen der Physik* 11 (1931) 649–678.
[4] S. Timoshenko, *Vibration Problems is Engineering*, Van Nostrand Princeton, New York, USA, 1937.
[5] S. Spinner, W.E. Teft, A method for determining mechanical resonance frequencies and for calculating elastic moduli from these frequencies, *Proceedings of the ASTM*, Vol. 61, 1961, 1221.
[6] ASTM, Standard test methods for dynamic Young's modulus, shear modulus and Poisson's ratio for advanced ceramics by impulse excitation of vibration, ASTM C, 1999, 1259–98.
[7] T. Lauwagie, H. Sol, G. Roebben, W. Heylen, Y. Shi, Validation of the Resonalyser method: an inverse method for material identification, *Proceeding of the International Seminars on Modal Analysis*, Leuven, Belgium, 2002.
[8] H. Sol, Identification of Anisotropic Plate Rigidities using Free Vibration Data, PhD Thesis, Vrije Universiteit Brussel, Belgium, 1986.
[9] H. Sol, J. De Visscher, H. Hongxing, J. Vantomme, P.W. De Wilde, La procedure Resonalyser, Revue des laboratoires d'essais 46, 1996.
[10] P.W. De Wilde, H. Sol, Anisotropic material identification using measured resonant frequencies of rectangular composite plates, *Fourth International Conference on Composite Structures*, Paisley College of Technology, Scotland, 1987, pp. 2317–2324.
[11] H. Sol, H. Hua, J. De Visscher, J. Vantomme, W.P. De Wilde, A mixed numerical/experimental technique for the nondestructive identification of the stiffness properties of fibre reinforced composite materials, *Journal of NDT&E International* 30 (2) (1997) 85–91.
[12] P. Pederson, P.S. Frederiksen, Identification of orthotropic material moduli by a combined experimental/numerical approach, *Measurement* 10 (1992) 113–118.
[13] L.R. Deobald, R.F. Gibson, Determination of elastic constants of orthotropic plates by a modal analysis/Rayleigh Ritz technique, *Journal of Sound and Vibration* 124 (1988) 269–283.
[14] E.O. Ayorinde, R.F. Gibson, Elastic constants of orthotropic composite materials using plate resonance frequencies, classical lamination theory and an optimised three mode Rayleigh formulation, *Composite Engineering* 3 (1993) 395–407.
[15] F. Moussu, M. Nivoit, Determination of the elastic constants of orthotropic plates by a modal analysis method of superposition, *Journal of Sound and Vibration* 165 (1993) 149–163.
[16] E.O. Ayorinde, Elastic constants of thick orthotropic composite plates, *Journal of Composite Materials* 29 (1995) 1025–1039.
[17] C.M. Mota Soares, M. Moreira de Freitas, A.L. Araujo, P. Pederson, Identification of material properties of composite specimens, *Composite Structures* 25 (1993) 277–285.
[18] P.S. Frederiksen, Estimation of elastic moduli in thick composite plates by inversion of vibrational data, *Proceedings of the Second International Symposium on Inverse Problems*, Paris, 1994, pp. 111–118.
[19] J. Cunha, Application des Techniques de Recalage en Dynamique a l'Identification des Constantes Élastiques des Matériaux Composites, Thèse PhD, Université de Franche-Comte, France, 1997.
[20] G.R. Liu, K.Y. Lam, X. Han, Determination of elastic constants of anisotropic laminated plates using elastic waves and a progressive neural network, *Journal of Sound and Vibration* 52 (2) (2002) 239–259.
[21] M.E. Friswell, J.E. Mottershead, *Finite Element Updating in Structural Dynamics*, Kluwer Academic Press, Dordrecht, 1999.
[22] H. Sol, C. Oomens, *Material Identification Using Mixed Numerical Experimental Methods*, Kluwer Academic Publishers, Dordrecht, 1997.
[23] R.M. Jones, *Mechanics of Composite Materials*, MacGraw-Hill, New York, USA, 1975.
[24] A.E.H. Love, *Mathematical Theory of Elasticity*, 4th Edition, Cambridge University Press, Cambridge, 1927.
[25] C.C. Chamis, *Structural Design and Analysis, Part 1, Composite Materials*, Vol. 7, Academic Press, New York, 1975.
[26] FEMtools Theoretical Manual, Dynamic Design Solutions, Leuven, 2002.
[27] R.L. Fox, M.P. Kapoor, Rates of changes of eigenvalues and eigenvectors, *American Institute of Aeronautics and Astronautics Journal* 6 (1968) 2426–2429.
[28] J. Beck, K. Arnorld, *Parameter Estimation in Engineering and Science*, Wiley, New York, USA, 1977.
[29] N. Imamovic, Validation of Large Structural Dynamics Models using Modal Test Data, PhD Thesis, Imperial College of Science, Technology & Medicine, London, 1998.